

USING THE TRANSIENT ELASTIC WAVE TECHNIQUE TO IMAGE THE DEFECT OF CONCRETE STRUCTURE

Tong Jian-Hua¹

¹ Department of Computer and Information Engineering, Hung Kuang University, Taichung, Taiwan, R.O.C

Abstract: Recently, great deals of civil engineering NDT techniques are developed for safety evaluation of concrete structures. With regard to the detection of the inner defects in concrete, image scanning scheme will provide very useful information. The traditional ultrasonic image shows good results on lab-cast concrete specimen, but it will not be practical on real structure owing to the high attenuation nature of ultrasound in concrete and the complexity of the equipment. In this paper, a new imaging method for defect scanning on in-situ structure will be proposed. It combines the well-known point-source/point-receiver measuring scheme and the SAFT technique for signal post-processing. The numerical simulation shows good result. The reflected signal could be enhanced with this method, the geometry and the location of defect could be clearly defined in the scanning image. It could possibly break through the limitation of scanning depth in traditional ultrasonic method and then be used to detect the inner defects in the in-situ structures.

Introduction: Among the present civil engineering NDT technologies^[1], the application based on the elastic wave theory always plays a very important role. The point-source/point-receiver scheme is especially suitable for the on-site civil infrastructure. It overcomes the limitation of transmission distance caused by the low output power nature of the traditional ultrasonic probe. Base on the theory of transient elastic wave, Wu et al.^[2,3] proposed a new method to measure the elastic wave velocity just on one surface of the in-situ structure and then use the result to obtain the elastic constants of the material non-destructively. Besides, he also proposed the method to measure the depth of the surface-breaking crack in concrete based on the diffraction nature of elastic wave^[4]. Liu et al.^[5] use the imaging technique to scan the depth of surface-breaking crack in reinforced concrete. By transforming the time domain signal into frequency domain to find the resonance frequency out, the impact-echo method could be used to detect the defects in specimen^[6-9]. The SASW (spectral analysis of surface wave)^[10] method utilizes the dispersive characteristic of elastic wave propagating in layer medium to check the pavement of roadway. When use the above mentioned methods to detect the inclusion in concrete infrastructures, however, it will be a very difficult task to analysis the received signal because of the complex reflection from the boundary and the lack of information from single signal. Applying the concept of phase array probe often used in medical ultrasound, it could be a reference to develop the new method finding out the defects with the scanning image of the concrete infrastructure^[11-14]. It is important to note that the energy of ultrasound decayed so quickly in concrete that the detectable depth will be limited seriously. Besides, the cost is too high and the size is too huge to be used as the NDT apparatus for civil infrastructure. It is in need of developing a new imaging method for the specific material.

SAFT (synthetic aperture focusing technique) is often used as a signal processing strategy in ultrasonic NDT. A pulse-echo probe is utilized to produce the ultrasonic wave and then received the reflected signal. Shifting and superposing the recorded signals, it could get the result as scanning with the phase array system and then enhance the S/N ratio of the received signals. The point-source/point-receiver scheme has been widely used in the field of NDT in civil engineering. It could produce high energy source to increase the detectable depth and also reduce the cost and size of the system. In this paper, the point-source/point-receiver scheme and SAFT image processing were combined to develop a new imaging method based on the transient elastic wave principle. From the FDM numerical simulation, it shows very good results. The defects could be clearly identified from the image. It shows the information of the location and the geometry of

defects. This result could be a practical and effective NDT method for defect imaging of civil infrastructure.

Principle of SAFT-imaging: In the traditional SAFT-imaging, the measurement is performed just with one ultrasonic probe. To match the present NDT measuring scheme in civil engineering, the measurement in this paper is replaced with a pair of point-source/point-receiver with a certain offset. Shown in fig.1 are the mechanism of measurement and the arrangement of imaging grid. The surface response $T_i(t)$ and the location of source and receiver S_i, R_i , should be recorded for the following process after the impact was performed.

The space should be divided into grids for imaging before the SAFT calculating begins. The image intensity $I(m,n)$ in each grid can be expressed as

$$I(m,n) = \frac{1}{N} \sum_{i=1}^N T_i(t_i) \quad (1)$$

$$t_i = \frac{|S_i I| + |I R_i|}{C_p} \quad (2)$$

Where N is the amount of signal and C_p is the longitudinal wave velocity.

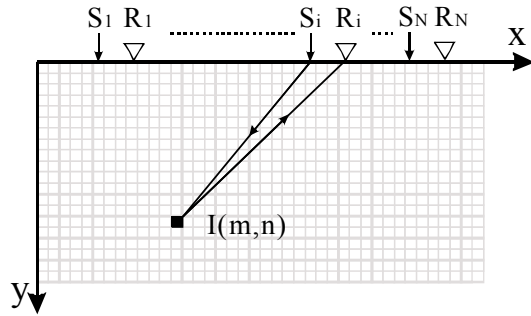


Fig.1 Grids and mechanism of measurement.

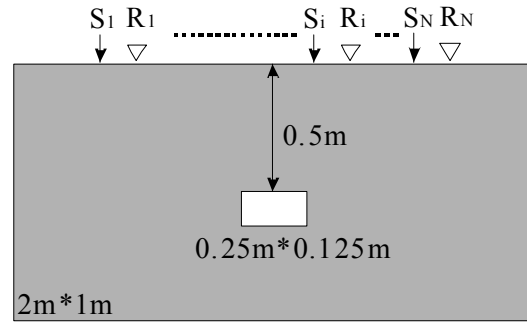


Fig.2 Arrangement of source/receiver pairs.

According to the elastic wave theory, the wave will be reflected at the interface between two media with different acoustic impedance. The reflection could be found on the time domain signal if it could be received by the transducer. In general case, however, there are so many reflected signals from the boundaries and defects that make the trace so complex and thus hard to identify the location of defect. Besides, the information of size and geometry are still invalid from one time domain signal. In SAFT-imaging process, it extracts the information not just from one signal but all the received signals to form the image. The intensity of each grid is summed with the corresponding point in all traces. The corresponding time of such point is the theoretical travelling time the wave propagating from source to grid point and then back to the receiver. With this process, the amplitude will be enlarged evidently when an interface exists right at the grid and it will appear as a bright point. In contrast, it will show a dark point in the image. The result will be similar to that scanned with a phased array system.

Results of numerical simulation: In this paper, a finite difference program for solving 2-D plane-strain problem was used as the numerical simulating tool to check the practicability of the new method mentioned above. The displacement signals were calculated out and then processed to form the SAFT image. A half $\sin^{3/2}t$ force-time function with $30\mu\text{s}$ contact time was used as a 6mm diameter steel ball impact. The signals of displacement and velocity on the surface are recorded after the calculation of finite difference program.

A. Displacement scanning image of single defect: The dimension and location of defect is shown in fig.2. There is a 0.25m*0.125m rectangular cavity in the 2m*1m concrete block. The longitudinal wave velocity of concrete is 3871m/s. Air is defined as the material of cavity. The impact point S_i of the first source-receiver pair is 0.5m away from the left boundary. The space between the source and the receiver is 0.1m. The signal was recorded at R_i when the source was applied at S_i . The displacement between two source-receiver pairs is 0.05m. The B-scan diagram of 20 displacement signals in y direction is shown as fig.3. The portion marked R is the signal of Rayleigh wave. B is the reflection from the bottom surface. These two signals are shown on all the recorded traces. The arrival time and the amplitude are almost the same. D is reflection from the defect. The receivers near the central region get much larger reflection from defect; others receive smaller reflection. The more the distance of the receiver from the central region, the smaller the amplitude of the reflection and also the larger the delay of the arrival time it is. Besides, the bottom reflection nearby exist some Rayleigh wave reflected from the side boundary in the signals recoded by the left and right side receivers.

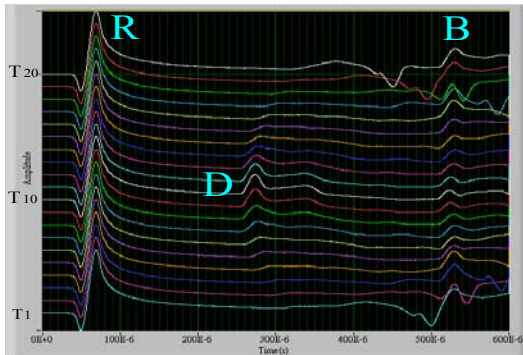


Fig.3 Displacement B-scan diagram.

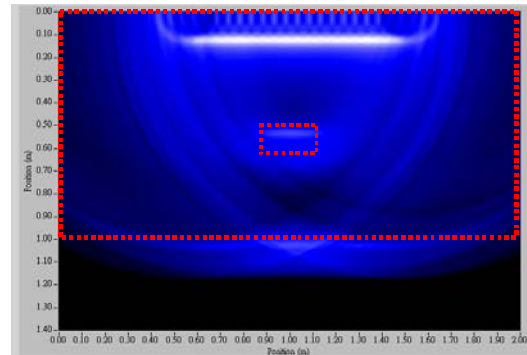


Fig.4 Image with single rectangular defect.

The algorithm of SAFT-imaging could be considered as another concept. The time axis of the received signal is transformed into the distance axis. The distance is the sum from source to index point and then back to receiver. In other words, each point on trace can produce an ellipse whose focal points are located at source and receiver. Superpose all the ellipses to get the image intensity field. As shown in fig.4 is the image composed with 20 traces in fig.3. The horizontal and vertical axes represent the actual dimension. The image intensity is mapping into the brightness. The stronger the intensity, the brighter it is. In this figure, a bright strip could be found near the surface. It doesn't represent the actually reflectional interface but the ghost image caused by Rayleigh wave. The bright strip in the center, as the portion marked with dotted rectangular, shows the existence of defect. It doesn't only show the location but also the length of the defect. It must be noted that only the surface of the defect could reflect the wave back to the receiver. Just the upper boundary of the defect could be found in image with this method. In fig.4, the larger rectangular marked with dotted line is the actual boundary of the specimen. The bottom boundary represented with a long bright strip could be also obviously found in the image. Two curves crossing at the center of the image are produced by the reflected Rayleigh wave.

It is worth to note that the amplitude of the Rayleigh wave is relatively larger than the reflected signals. The dynamic range of the image intensity is too large that the contrast of the defect image will be compressed. Remove the value of the region above 0.2m of the surface and redraw the image as shown in fig.5. The contrast of the remnant image increases evidently after the influence of Rayleigh wave was removed. The location and geometrical properties of the defect and bottom boundary could be obtained clearly from the enhanced image.

As shown in fig.6 is the scanned image of a concrete specimen with a 0.2m diameter circular hole in it. The size and location of the hole is marked with the dotted circle. From the result, not

only the location but also the shape of the upper part of the defect could be clearly obtained. It is obvious that the result obtained by the method in this paper is much easier to be read than the traditional B-scan diagram.

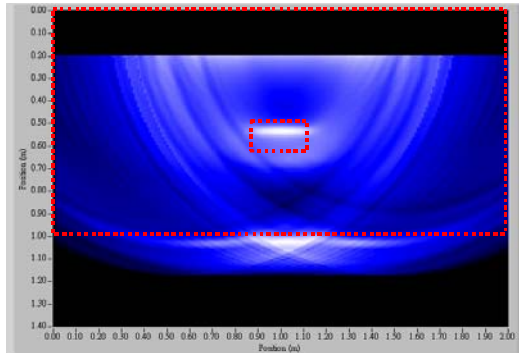


Fig.5 Image with Rayleigh wave removed.

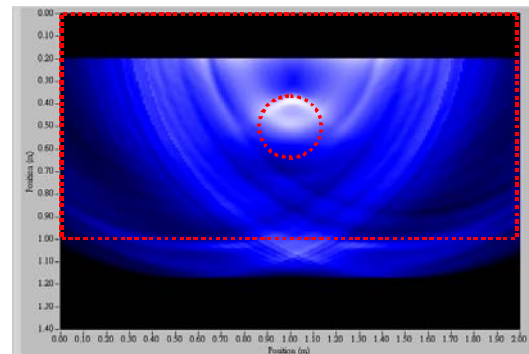


Fig.6 Image with single circular defect.

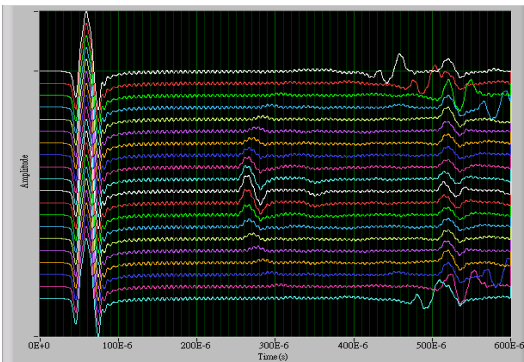


Fig.7 Velocity B-scan diagram.

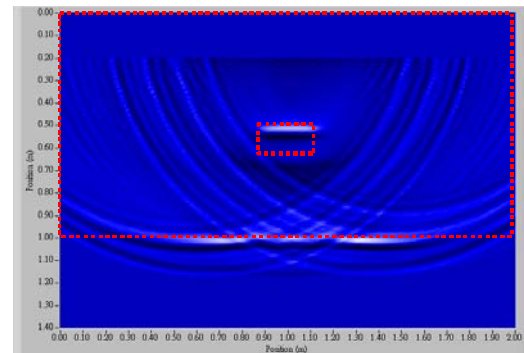


Fig.8 Velocity image with single rectangular defect.

B. Velocity scanning image of single defect: Fig.7 is the B-scan diagram of 20 velocity signals measured on the specimen in fig.2. The velocity signals were removed the influence of Rayleigh wave and then processed with the SAFT method to form the image as shown in fig.8. When compare the velocity scanning image with the displacement scanning image, it could be found that the contrast of the image is higher and thus the location and shape is easier to define. In addition, the ghost image is fewer. The reason for this is not hard to see: it is that the reflected velocity signals in fig.7 have both positive and negative value. The value of the grid at the interface will increase owing to the in-phased superpose; otherwise it may be eliminated owing to the out-of-phased superpose. On the contrary, there are still some bright images near the defect in fig.5. The reflected displacement signals from defect in fig.3 are similar with the force-time function of the source: the signals are all positive. The value could not be eliminated by superpose even the out-of-phased superposing. Nevertheless, the displacement scanning image still can show the information of the defect in specimen. In practical application, the image could be generated according to the type of receiver used in the measurement.

C. Multi-defect scanning image: Fig.9 is the displacement B-scan diagram of a specimen with two rectangular holes in it. Take the portion before $600\mu s$ of these 20 signals into the SAFT processing and then form the image as shown in fig.10(a). All the same, the location and shape are marked with dotted rectangular. From the image, the upper boundary of the two defects could be clearly identified. The shape and location of the bright zone are consistent with the defects. The bottom of the specimen could also be found in the image. The bottom reflection is not as clear as that in fig.5. It's comes form that most of the energy are reflected back by the defects.

Only few energy could arrive the bottom boundary and then back to the receiver. It is worth noting that these two defects could not be distinguished directly from the traditional B-scan diagram even though the reflected wave could be found in the traces. The image processing technique proposed in this paper makes the identification of the defect in image more easily.

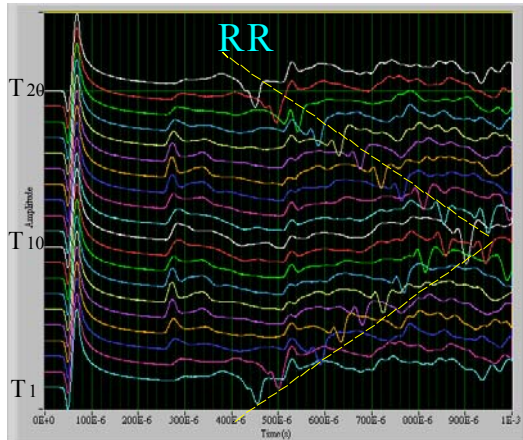


Fig.9 Displacement B-scan diagram.

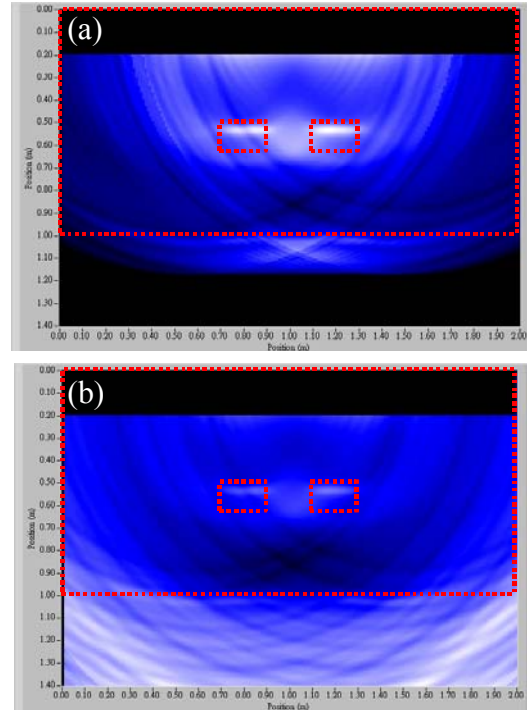


Fig.10 Image of double rectangular defects.

D. The influence of the signal length: Fig.10(b) is the SAFT-imaging generated from 20 traces of fig.9. It is almost the same as fig.10(a) except the signal length. It takes the full-length traces into the process. The image could still show the information of these two defects. But some ghost image could be found beneath the bottom of specimen. It comes from the reflected Rayleigh wave on the lateral boundary as marked RR in fig.9. Reflected Rayleigh wave with larger amplitude induces unwanted bright zone in the scanning image when longer signal is taken into process. It will interfere with the defect judgment of the image. The influence of the signal length should be carefully taken into consideration when using the SAFT-imaging method.

Conclusions: When mention about NDT in civil engineering, point-source/point-receiver scheme, using high energy elastic wave, is a good solution to measure the reflected signal from the inclusion deep beneath the surface. On lack of useful information, however, it is hard to identify the exact location and shape of the defect with single received signal. The traditional ultrasonic method could be used to scan just the shallow defects owing to the low wave energy. Besides, the cost and complexity of such equipment seriously limits its application for in-situ use. In this paper, it takes advantages of the point-source/point-receiver technique and SAFT-imaging process and then proposes a new method to detect the defects of the in-situ structures by imaging. It makes the elastic wave propagate longer using the point-source mechanism and thus the receiver could detect the signals reflected from deep inclusion. The SAFT process could be used to achieve the effect as scanning with a phased array system by post-processing the recorded signals but no bulky apparatus is needed. It extracts the useful information in all signals to enhance the S/N ratio of the image and expose the location and shape of the defects. What is important is that the imaging method proposed here could adopt the well developed apparatus of

the elastic-wave-based technology. It is not needed to spend lots of money to develop new equipment. From the numerical result done in this paper, it shows great potential on imaging the defects of concrete structures by using the transient elastic wave technique. It will be a breakthrough on civil-engineering NDT technology, if the practicability is proved by the experiment performed on real-size specimen in the future.

Acknowledgement: The author thanks the National Science Council of ROC for the financial support of this research through the grant NSC92-2211-E-241-007-.

References:

1. Malhotra, V. M. and Carino, N. J. (1991), CRC Handbook on Nondestructive Testing of Concrete, CRC Press, Inc., pp.169-188.
2. Wu, T. T. and Fang, J. S. (1997), "A new method for measuring concrete elastic constants using horizontally polarized conical transducers," J. Acoust. Soc. Am., Vol. 101, No.1, pp. 330-336.
3. Wu, T. T., Fang, J. S., Liu, G. Y. and Kuo, M. K. (1995), "Detection of elastic constants of a concrete specimen using transient elastic waves," J. Acoust. Soc. Am., Vol. 98, No. 4, pp. 2142-2148.
4. Wu, T. T., Fang, J. S., and Liu, P. L. (1995), "Detection of the Depth of a Surface-breaking Crack Using Transient Elastic Waves", J. Acoust. Soc. Am., Vol. 97, pp.1678-1686.
5. P.-L. Liu, K.-H Lee, T.-T. Wu, M.-K. Kuo (2001), "Scan of Surface-opening Cracks in Reinforced Concrete Using Transient Elastic Waves", NDT & E International, Vol. 34, pp. 219-226.
6. ASTM (1990), Annual Book of ASTM Standard, Philadelphia, PA: Concrete and Aggregates, 1990, C597-83, Vol. 04.02, pp. 291-293. N.J. Carino and M. Sansalone, "Detection of Voids in Grouted Ducts Using the Impact-Echo Method," ACI Materials Journal, 89, (3), 296-303 (1992).
7. Carino, N. J., Sansalone, M. and Hsu, N. (1986). "A point source point receiver pulse-echo technique for flaw detection in concrete," ACI Journal, proceeding, Vol. 83, pp.199-208.
8. Sansalone, M. and Carino, N. J. (1986), "Impact-Echo: A method for flaw detection in concrete using transient stress wave," Report No. NBSIR 86-3452, National Bureau of Standard, Washington, D.C./PB 87-10444/AS, National Technical Information Service, Springfield.
9. Carino, N.J., and Sansalone, M. (1992), "Detecting Voids in Metal Tendon Ducts Using the Impact-Echo Method," ACI Materials Journal, Vol. 89, No. 3, pp. 296-303.
10. Nazarian, S. and Desai, R. (1993), "Automated surface wave method: Field testing," J. Geotechnical Engineering, Vol. 119, No. 7, pp. 1094-1111.
11. Oral Büyükoztürk (1998), "Imaging of Concrete Structures," NDT & E International, Vol.31, No.4, pp. 233-243.
12. Young-Fo Chang, Chung-Yue Wang and Chao-Hui Hsieh (2001), "Feasibility of Detecting Embedded Cracks in Concrete Structures by Reflection Seismology," NDT & E International, Vol.34, pp. 39-48.
13. Kevin L. Rens, P.E., Associate Member, ASCE, David J. Transue and Michael P. Schuller, P.E., Member, ASCE (2000), "Acoustic Tomographic Imaging of Concrete Infrastructure," Journal of Infrastructure system, Vol.6, No. 1, pp. 15-23.
14. Masayasu Ohtsu and Takeshi Eatanabe (2002), "Stack Imaging of Spectral Amplitudes Based on Impact-echo for flaw Detection," NDT & E International, Vol.35, pp. 189-196.
15. S. R. Doctor, T. E. Hall and L. D. Ried (1986), "SAFT- The Evolution of a Signal Processing Technology for Ultrasonic Testing," NDT Int., Vol. 19, pp. 163-167.
16. John Waszak and Reinhold Ludwig (1990), "Three-Dimensional Ultrasonic Imaging Employing a Time-Domain Synthetic Aperture Focusing Technique," IEEE Transactions on Instrumentation and Measurement, Vol. 39, No. 2, pp. 441-444.

17. Seth D. Silverstein and Lewis J. Tomas (1993), "Analytical Comparison of sensor Processing Enhancements for NDT Synthetic Aperture Ultrasonic Imaging," IEEE Transactions on Image Processing, Vol. 2, No. 1, pp. 60-67.
18. Young-Fo Chang and Chen-I Hsieh (2002), "Time of flight Diffraction Imaging for Double-Probe Technique," IEEE Transactions on Ultrasonics, Ferroelectrics, and Frequency Control, Vol. 49, No. 6, pp. 776-783.
19. M. Krause, F. Mielentz, B. Milman, W. Müller, V. Schmitz and H. Wiggerhauser (2001), "Ultrasonic Imaging of Concrete Members Using an Array System," NDT & E International, Vol.34, pp. 403-408.